INFECTION AND IMMUNITY, May 2007, p. 2110–2119 Vol. 75, No. 5
0019-9567/07/$08.00+0 doi:10.1128/IAI.01739-06

Invasion and Persistence of *Mycobacterium avium* subsp. *paratuberculosis* during Early Stages of Johne's Disease in Calves[▽]

Chia-wei Wu,[1] Michael Livesey,[2] Shelly K. Schmoller,[1] Elizabeth J. B. Manning,[1] Howard Steinberg,[1] William C. Davis,[3] Mary Jo Hamilton,[3] and Adel M. Talaat[1]*

The Laboratory of Bacterial Genomics, Department of Pathobiological Sciences,[1] and Department of Surgical Sciences,[2] University of Wisconsin, Madison, Wisconsin 53706, and Department of Veterinary Microbiology and Pathology, Washington State University, Pullman, Washington[3]

Received 31 October 2006/Returned for modification 19 December 2006/Accepted 2 February 2007

Infection with *Mycobacterium avium* subsp. *paratuberculosis* causes Johne's disease in cattle and is a serious problem for the dairy industry worldwide. Development of models to mimic aspects of Johne's disease remains an elusive goal because of the chronic nature of the disease. In this report, we describe a surgical approach employed to characterize the very early stages of infection of calves with *M. avium* subsp. *paratuberculosis*. To our surprise, strains of *M. avium* subsp. *paratuberculosis* were able to traverse the intestinal tissues within 1 h of infection in order to colonize distant organs, such as the liver and lymph nodes. Both the ileum and the mesenteric lymph nodes were persistently infected for months following intestinal deposition of *M. avium* subsp. *paratuberculosis* despite a lack of fecal shedding of mycobacteria. During the first 9 months of infection, humoral immune responses were not detected. Nonetheless, using flow cytometric analysis, we detected a significant change in the cells participating in the inflammatory responses of infected calves compared to cells in a control animal. Additionally, the levels of cytokines detected in both the ileum and the lymph nodes indicated that there were TH1-type-associated cellular responses but not TH2-type-associated humoral responses. Finally, surgical inoculation of a wild-type strain and a mutant *M. avium* subsp. *paratuberculosis* strain (with an inactivated *gcpE* gene) demonstrated the ability of the model which we developed to differentiate between the wild-type strain and a mutant strain of *M. avium* subsp. *paratuberculosis* deficient in tissue colonization and invasion. Overall, novel insights into the early stages of Johne's disease were obtained, and a practical model of mycobacterial invasiveness was developed. A similar approach can be used for other enteric bacteria.

Johne's disease (JD) or paratuberculosis in cattle is caused by *Mycobacterium avium* subsp. *paratuberculosis*. Virtually all ruminants are believed to be susceptible to infection with this organism, which causes severe economic losses estimated to be around $200 to $250 million a year for the dairy industry in the United States alone (19). Worldwide, the prevalence of the infection can range from 3 to 4% in herds (e.g., in England) (4) to as much as 50% in herds (e.g., in Wisconsin and Alabama) (6, 14). A recent report by members of the National Research Council on the status of JD stressed the need to fill several gaps in our knowledge associated with the pathophysiology, immunology, and control of JD (7). JD research is hampered by the low growth rate of *M. avium* subsp. *paratuberculosis* and the lack of a reliable animal model to investigate host-pathogen interactions. Despite the introduction of molecular protocols to facilitate JD diagnosis (11, 39), the tools that are available are unreliable for detection of infected cows, especially cows in the early stages of infection (5). Currently, no effective treatment regimen is available, and the control strategies for afflicted herds are based on testing and culling infected animals (16, 24). More effort is needed to better understand the pathogenesis of JD and to develop an effective control strategy. A key aspect of JD pathogenesis is related to the early events of mycobacterial colonization of the intestine. So far, the mechanisms responsible for intestinal invasion and persistence of *M. avium* subsp. *paratuberculosis* are poorly understood (41). Using the calf model of JD, we thoroughly examined the very early steps of intestinal colonization and invasion, as well as subclinical stages of JD. Detailed knowledge of the early host-pathogen interactions could provide the information needed to develop an efficient strategy for controlling *M. avium* subsp. *paratuberculosis* infections.

Cattle infected with *M. avium* subsp. *paratuberculosis* usually suffer from chronic diarrhea, weight loss, low milk yield, and increased morbidity. The incubation period of JD is usually 2 to 4 years, during which shedding of *M. avium* subsp. *paratuberculosis* is intermittent (45). Clinically affected cows can shed 10^6 to 10^8 CFU/g of fecal material, thus contaminating the environment and spreading the infection to newborn calves, and the estimated infectious dose is $\sim 10^3$ CFU/animal (45). To reduce the cost associated with investigation of JD in cattle, several nonbovine infection models have been used, none of which provides a complete clinical picture of JD. For example, to simulate the granulomatous enteritis aspect of JD, both immune-competent (38) and immune-compromised (12, 25) mouse models have been successfully employed to model the chronic features of *M. avium* subsp. *paratuberculosis* infection. In another attempt to develop an animal model in which the

* Corresponding author. Mailing address: The Laboratory of Bacterial Genomics, Department of Pathobiological Sciences, University of Wisconsin-Madison, 1656 Linden Drive, Madison, WI 53706-1581. Phone: (608) 262-2861. Fax: (608) 262-7420. E-mail: atalaat@wisc.edu.
▽ Published ahead of print on 12 February 2007.

course of the disease is shorter, goats were used to evaluate the subclinical phase of JD and to investigate the type of T lymphocytes recruited during vaccination (33, 42). Interestingly, cell-mediated immunity was first detected 9 weeks following oral infection of goats with *M. avium* subsp. *paratuberculosis*, while antibodies were detected only at later times after infection (15 to 20 weeks) (33). A similar result was also obtained following oral inoculation of goats with *M. avium* subsp. *paratuberculosis*-infected tissues (23), indicating the important role played by cell-mediated immunity in the control of early stages of JD. To develop a better model for early stages of JD, neonatal calves were infected via the oral route (43), as well as via tonsillar crypt deposition (40). In both models, infection with virulent isolates of *M. avium* subsp. *paratuberculosis* successfully elicited immune responses but did not induce clinical signs of JD, such as diarrhea and intestinal lesions, even after prolonged infection. Further characterization of the calf model is needed to address questions related to intestinal colonization, invasion, and the spread of the infection.

To study the invasion of JD, Momotani et al. examined intestinal loops of calves within hours after inoculation of *M. avium* subsp. *paratuberculosis* and showed that M cells were the main entry cells for *M. avium* subsp. *paratuberculosis* (22). A subsequent analysis of the murine model indicated that enterocytes rather than M cells are involved in *M. avium* subsp. *paratuberculosis* entry (27). In this report, we describe a surgical approach for investigating the early stages of JD (up to 9 months) and for understanding the changes in host immunity during this important stage of infection. Surprisingly, the mycobacterial invasion of intestinal cells was very rapid, and a considerable level of infection was maintained in the mesenteric lymph nodes, as well as in the intestine. Unlike humoral immunity, cellular responses to infection were readily detected in infected animals. Finally, the calf model developed was used to evaluate the colonization and invasiveness of an attenuated *M. avium* subsp. *paratuberculosis* mutant, indicating that this model can be used to study virulence traits of *M. avium* subsp. *paratuberculosis*.

MATERIALS AND METHODS

Animals. Seven male Holstein calves that were 14 to 21 days old were purchased from a dairy herd that had been JD free for the previous 5 years (Preventive Level A Wisconsin Dairy Herd). Sera and fecal samples collected from the calves and their dams were examined and were demonstrated to be negative for evidence of *M. avium* subsp. *paratuberculosis* infection by an IDEXX enzyme-linked immunosorbent assay (ELISA) (21) before inclusion in the study. All animals were housed in isolation under biosafety level 2 conditions and were cared for according to our protocol approved by the Institutional Animal Care and Use Committee, University of Wisconsin-Madison. All animal waste and disposable utensils used throughout the project were autoclaved before disposal. The animals were monitored daily for any behavioral changes or the appearance of signs consistent with JD.

Bacterial strains. *M. avium* subsp. *paratuberculosis* strains K-10 and ATCC 19698 were grown in Middlebrook 7H9 broth (Difco, Sparks, MD) supplemented with 0.5% glycerol, 0.05% Tween 80, 2 μg/ml of mycobactin J (Allied Monitor, Fayette, MO), and 10% ADC (2% glucose, 5% bovine serum albumin fraction V, 0.85% NaCl) at 37°C (46). When a Δ*gcpE* mutant (an insertional mutant) (30) derived from strain ATCC 19698 was grown, kanamycin (50 μg/liter) was added to the medium. For animal infections, bacterial cultures were grown to an optical density at 600 nm of 1.0, and cells were harvested by centrifugation at 3,200 × *g* and resuspended in an equal volume of phosphate-buffered saline (PBS). Middlebrook 7H10 agar (Difco) supplemented with mycobactin J was used for serial plating of bacterial cultures or infected tissues to estimate colony counts. In our hands, the lowest level that could be detected in infected tissues was 20 CFU/g of tissue. Fecal samples collected from infected and control inoculated animals were processed for culturing using the BACTEC and MGIT systems (BD, Franklin Lakes, NJ) as described previously (8).

Surgical intervention. All surgeries were performed at the Veterinary Medical Teaching Hospital, School of Veterinary Medicine, University of Wisconsin-Madison, using standard aseptic surgical techniques. Before surgical inoculation of *M. avium* subsp. *paratuberculosis*, calves were restrained in left lateral recumbency under general anesthesia. The abdominal cavity of each calf was entered through a vertical incision made through the skin and muscle layers in the middle of the right paralumbar fossa. The cecum and ileum were exposed and isolated from the contents of the abdominal cavity with saline-moistened sponges. Approximately 10 cm of the distal jejunum and proximal ileum was identified, and the lumen was occluded by application of intestinal clamps at the proximal and distal ends of the segment. The clamps were applied from the antimesenteric surface to avoid occlusion of the mesenteric blood supply. A 10-ml inoculum containing either PBS (controls) or 10^7 to 10^8 *M. avium* subsp. *paratuberculosis* CFU/ml was then injected into the lumen of the occluded segment of the bowel. After 1 to 2 h of occlusion, a regional lymph node from the ileocecal mesentery and full-thickness sections of the bowel were harvested from the jejunum immediately proximal to the occluded segment. Sections of the bowel were harvested by making a full-thickness bilateral elliptical incision, approximately 1 cm long, longitudinally through the antimesenteric surface of the bowel. The color of the occluded segment was monitored to ensure that blood vascularization was maintained despite the intestinal clamps. To minimize the risk of luminal stricture, the defect was closed by suturing the bowel in a transverse plane. The bowel was liberally lavaged with sterile polyionic fluids, and then the bowel and occluding clamps were returned to the abdominal cavity. The abdominal incision was closed, and the animal was allowed to recover from anesthesia.

Following surgery, calves were monitored twice daily, and fecal samples were cultured every day for 7 days and then weekly until termination of the experiment. Beginning 1 month postinoculation and then at intervals no greater than bimonthly, operations were performed to obtain a full-thickness section of bowel from the terminal ileum and a regional lymph node of each calf. At 4 days postinfection, one of the infected calves was sacrificed so that early samples could be collected from organs that are inaccessible by laparoscopy. The rest of the animals were sacrificed 6, 7 (control), 8, and 9 months following infection. At necropsy, tissues were collected from the ileum, three sections of the jejunum, the duodenum, and at least three mesenteric lymph nodes, as well as two sections of the liver, spleen, kidney, and lungs. All biopsy samples were analyzed by culturing on Middlebrook 7H10 medium and by standard histological examination.

Competitive index assay. Both *M. avium* subsp. *paratuberculosis* wild-type strain ATCC 19698 and its isogenic Δ*gcp* mutant were grown to an optical density at 600 nm of 1.0. Before inoculation of animals, cultures were centrifuged and resuspended in PBS, and equal volume of cultures were mixed. Ten milliliters of the culture mixture was inoculated into an anesthetized calf as described above. Following infection (1 to 2 h), samples were obtained from the mesenteric lymph nodes, small intestine, liver, and spleen. Duplicate tissue homogenates were processed for bacterial counting using Middlebrook 7H10 agar in the presence or absence of kanamycin. The identities of bacterial colonies were verified using PCR (see below). The percentages of wild-type and mutant counts were used in the following formula to calculate the competitive index of virulence (CIV) (26): CIV = (output CFU of mutant/output CFU of wild type)/(input CFU of mutant/input CFU of wild type).

Immune assays with infected animals. Blood samples (10 to 15 ml) were also collected weekly for the first month following inoculation and then biweekly until the end of the experiment. Blood was collected from the jugular vein and centrifuged, and the resulting sera were tested within 24 h of collection. Each serum was tested for antibody against *M. avium* subsp. *paratuberculosis* using an IDEXX ELISA kit as described previously (21). The results were considered positive or negative based on the description provided by the manufacturer. For flow cytometric analysis, 250 to 500 ml of acid citrate dextrose blood samples were collected from the jugular vein of infected and control animals before sacrifice and processed for flow cytometric analysis to obtain a profile for the changes in immune cells following *M. avium* subsp. *paratuberculosis* inoculation. Most of the primary antibodies to cellular surface antigens were obtained from the Washington State University Monoclonal Center; the only exception was AKS1, which was a gift from Anne Storset, Norwegian School Veterinary Science. The panel of monoclonal antibodies (MAbs) used for flow cytometric analysis is shown in Table 1. The peripheral blood mononuclear cells (PBMC) used in cultures and flow cytometric analysis were obtained from the buffy coat fractions of blood separated by density gradient centrifugation with Accu-Paque (density, 1.086 g/ml; Accurate Chemical & Scientific Corp., Westbury, NY). The

TABLE 1. MAbs that were used in the flow cytometric analysis[a]

MAb	Immunoglobulin isotype	Specificity
AKS1	G1	NKp46
MUC2A	G2a	CD2
ILA-11A	G2a	CD4
CACT187A	G1	CD4
7C2B	G2a	CD8
CACT80C	G1	CD8α
GB21A	G2b	δγ T δ chain specific
GC44A1	G3	CD45R0
CACT116A	G1	CD25
CACT114A	G2b	CD26
CACT200A	G1	ACT1
LCTB6A	G1	ACT9
IL-A77	M	CD71
GB110A	M	ACT16
CACT195A	M	ACT27
CACT216A	M	ACT28
CACT225A	G1	ACT29
CACT185A	G1	ACT30
CACT152A	M	ACT31
CACT191A	M	ACT32
H34A	G2b	MHC II

[a] See reference 18.

PBMC were washed several times in PBS containing 20% acid citrate dextrose to remove excess platelets and then used in culture and flow cytometric analyses as described previously (18).

Combinations of MAbs were used in three-color analyses. All MAbs were used at a concentration of 15 μg/ml. The same combinations of MAbs were used for labeling cells at the initiation and after 6 days of culture. A FACSort flow cytometer equipped with argon and red lasers, a Macintosh Quadra computer, and the Cell Quest software (Becton Dickinson Immunocytometry Systems, San Jose, CA) were used to collect data. The FCS Express software (De Novo Software, Thornton, Ontario, Canada) was used to analyze the data, as described previously (18).

PPD skin test. To examine the development of cell-mediated immunity, animals were inoculated with purified protein derivatives (PPD) prepared from *Mycobacterium avium* subsp. *avium* (a generous gift from Mike Collins, University of Wisconsin-Madison) in the skin fold of the tail. All testing was performed using animals that were inoculated 3 to 4 months after experimental infection with *M. avium* subsp. *paratuberculosis*. One milliliter of PPD per animal was administered via intradermal injection using 18-gauge needles. At 48 h following infection, induration and the thickness of the skin fold were measured using a standardized caliper.

PCR analysis of *M. avium* subsp. *paratuberculosis* colonies. To determine the identities of the colonies that grew on the colony counting plates, a PCR amplification protocol was used. Several colonies (n = 10 to 20) were picked, and each colony was resuspended in 10 μl of PBS. After boiling for 10 min, 2 μl of supernatant was amplified in the presence of either IS*900* or kanamycin-resistant gene-specific primers (Table 2), using the following conditions: 95°C for 5 min, 35 cycles of 94°C for 30 s, 59°C for 30 s, and 72°C for 45 s, and a final extension at 72°C for 7 min. All amplification products were visualized on 2% agarose gels stained with ethidium bromide.

Quantitative real-time PCR (RT-PCR). Samples of total RNA were extracted from infected calf tissues and treated with Turbo DNA free (Ambion, Austin, TX) for 1 h at 37°C. The extracted total RNA was used as a template for a standard reverse transcription reaction in the presence of random hexamer oligonucleotides as described previously (36). The cDNA generated served as a template for quantitative PCR in the presence of gene-specific primers (Table 2) and SYBR green dye (28, 29). For each amplification (ABI7700; Applied Biosystems), the calculated cycle threshold (C_T) for each gene amplicon was normalized to the C_T of the β-actin gene (amplified from the same sample) before calculation of the fold change from in vivo and in vitro samples. The following formula was used to estimate the fold change: fold change $= 2^{-\Delta\Delta C_T}$, where $\Delta\Delta C_T$ for gene j is $(C_{T,j} - C_{T,\beta\text{-actin}})_{\text{infected}} - (C_{T,j} - C_{T,\beta\text{-actin}})_{\text{control}}$. The melting curves for all reactions were examined to identify primer-dimer formation and to ensure that the amplicons of all the genes were uniform.

Histopathology. The tissue sections used for histological analysis were collected and preserved in 10% neutral buffered formalin. Tissues embedded in paraffin were prepared for microtome sectioning (3 to 5 μm) and for staining with standard hematoxylin and eosin or acid-fast staining as described previously (37). Two independent pathologists examined stained slides to score changes in the inflammatory response using a scale that ranged from 0 to 5. A score of 1 indicated that there was a limited inflammatory response, while a score of 5 indicated that there were multiple granulomas in more than three representative microscopic fields.

Statistical analysis. Student's t test was used to evaluate differences in bacterial colonization among different tissues during 9 months of infection. Analysis of variance followed by the Tukey-Kramer multiple-comparison test was used to evaluate the flow cytometric data for infected and control animals (De Novo FCS Express software).

RESULTS

Fate of *M. avium* subsp. *paratuberculosis* following intestinal deposition and persistent infection. Clinically, all animals survived the initial infection and the repeated surgical interventions without untoward effects. Daily observations of infected animals did not reveal any differences between their behavior and food intake and the behavior and food intake of an infection-free, control calf. Additionally, routine clinical inspection of infected animals did not reveal any clinical signs of systemic infection. Interestingly, culturing of mesenteric lymph nodes following intestinal inoculation showed that there were significant levels of colonization in all animals examined within 1 to 2 h postinfection (lymph nodes were collected following 1 to

TABLE 2. Primers used in this study

Primer	Gene	Sequence (5′→3′)
AMT10	*M. avium* subsp. *paratuberculosis*, IS*900*, forward	TACCTTTCTTGAAGGGTGTTCGGGG
AMT11	*M. avium* subsp. *paratuberculosis,* IS*900*, reverse	TTGTGCCACAACCACCTCCG
AMT272	Kanamycin, forward	TTAAATTCCAACATGGATGCTGATTT
AMT273	Kanamycin, reverse	GGCAAAAGATTATGCATTTCTTTCCA
AMT769	Bovine, IL-4, forward	TTGGAATTGAGCTTAGGCGTAT
AMT770	Bovine, IL-4, reverse	CCAAGAGGTCTTTCAGCGTACT
AMT771	Bovine, INF-γ, forward	GATTCAAATTCCGGTGGATG
AMT772	Bovine, INF-γ, reverse	TTCTCTTCCGCTTTCTGAGG
AMT773	Bovine, TNF-α, forward	AACATCCTGTCTGCCATCAAG
AMT774	Bovine, TNF-α, reverse	GGAAGACTCCTCCCTGGTAGAT
AMT775	Bovine, IL-12, forward	CAAAAAGGAAGATGGAATTTGG
AMT776	Bovine, IL-12, reverse	CCAGAATAATCCTTTGCCTCAC
AMT777	Bovine, β-actin, forward	ATGCTTCTAGGCGGACTGTTAG
AMT778	Bovine, β-actin, reverse	ACAAATAAAGCCATGCCAATCT

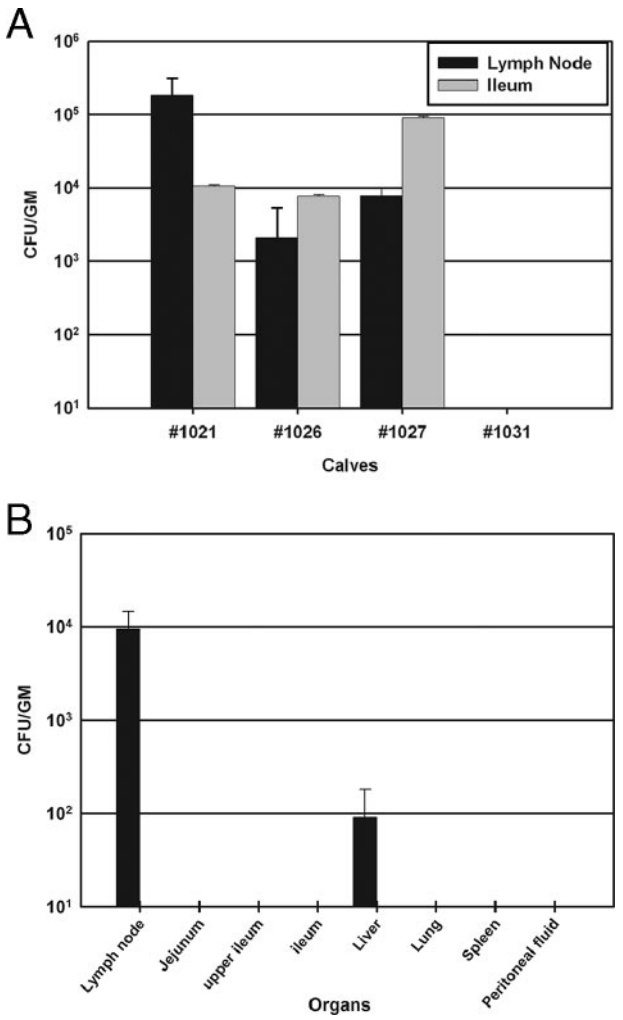

FIG. 1. Bacterial colonization of calves infected with *M. avium* subsp. *paratuberculosis* at very early times following infection. (A) Colonization of the ileum and mesenteric lymph nodes 1 h after inoculation of 10^9 CFU/animal for calf 1021 and inoculation of 10^8 CFU/animal for calves 1026 and 1027. (B) Colonization of calf 1022 organs 4 days after infection with 10^{10} CFU *M. avium* subsp. *paratuberculosis*. The error bars indicate standard errors of the means.

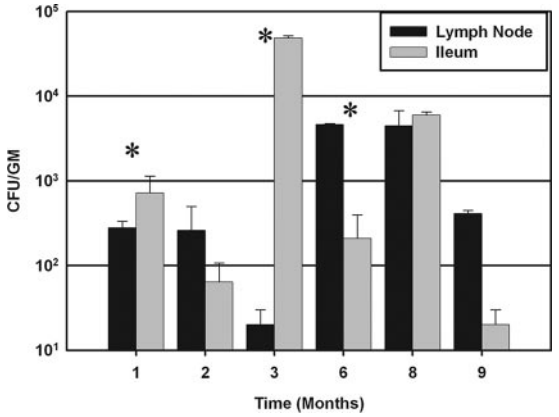

FIG. 2. Differential colonization of calf tissues during persistent infection with *M. avium* subsp. *paratuberculosis*. The colony counts in both the ileum and the mesenteric lymph nodes were determined for 9 months following surgical infection with *M. avium* subsp. *paratuberculosis* (10^9 CFU/calf). The error bars indicate standard errors of the means. An asterisk indicates that the levels of colonization of the lymph nodes and the ileum are significantly different, as determined by Student's *t* test ($P < 0.05$).

2 h of luminal deposition), indicating that there was rapid invasion and migration of *M. avium* subsp. *paratuberculosis* bacilli from the intestine to the mesenteric lymph nodes (Fig. 1A). In fact, a large inoculum (10^9 CFU/animal) resulted in a higher level of colonization of the lymph nodes than a smaller inoculum (10^8 CFU/animal) resulted in, implying that the intestinal invasion movement of the organisms to the lymph nodes is a dose-dependent process. Also, culturing of fecal samples in the first 3 days postinfection revealed shedding of *M. avium* subsp. *paratuberculosis* in fecal samples of infected animals, while the control calf remained fecal culture negative. Bacterial shedding at this early stage of infection could have represented "passive shedding" from the initial inoculation.

To ensure that the infectious dose was suitable and to examine very early predilection sites for *M. avium* subsp. *paratuberculosis* following inoculation, a complete postmortem examination was conducted for a calf sacrificed 4 days postinfection. When intestinal tissue of the sacrificed calf was examined, a slight edematous enlargement of the intestinal wall was noticed, while in the remaining organs there were no alterations. However, the colony counts for mesenteric lymph node and liver sections revealed a significant level of bacterial colonization (Fig. 1B). There were not detectable levels of *M. avium* subsp. *paratuberculosis* in other tissues, including the spleen, lung, and peritoneal fluid, indicating that these organs were not colonized in the first few days following infection. Surprisingly, in repeated attempts to culture intestinal tissues (ileum and jejunum) we did not detect *M. avium* subsp. *paratuberculosis* bacilli in samples collected 4 days postinfection. Histological analysis of an *M. avium* subsp. *paratuberculosis*-inoculated calf revealed no specific lesions that could be attributed to the *M. avium* subsp. *paratuberculosis* inoculation.

On the organ level, the fate of *M. avium* subsp. *paratuberculosis* bacilli following an initial infection is largely unknown. For example, following enteric infection with *M. avium* subsp. *paratuberculosis*, it is not known whether *M. avium* subsp. *paratuberculosis* bacilli remain mainly in the intestine or colonize other body organs. To address this question, we devised a staggered sampling strategy in which infected animals were either sampled by laparotomy or sacrificed at different times so organ colonization could be analyzed monthly. In addition, the number of surgeries performed could be minimized so that there were only two surgeries per calf. Interestingly, following the early infection stage (first 4 days postinfection) and beginning 30 days postinfection, *M. avium* subsp. *paratuberculosis* bacilli were cultured only from the ileum and lymph node samples (detection limit, 20 CFU/g) and not from other tissues (duodenum, liver, spleen, lung, kidney, and peritoneal fluid). *M. avium* subsp. *paratuberculosis* bacilli were retrieved from the jejunum of only one calf, which was sacrificed 8 months postinfection (data not shown). The considerable levels of *M. avium* subsp. *paratuberculosis* detected in ileum and lymph node samples at all the times examined (1 to 9 months) indicated that *M. avium* subsp. *paratuberculosis* preferred to colo-

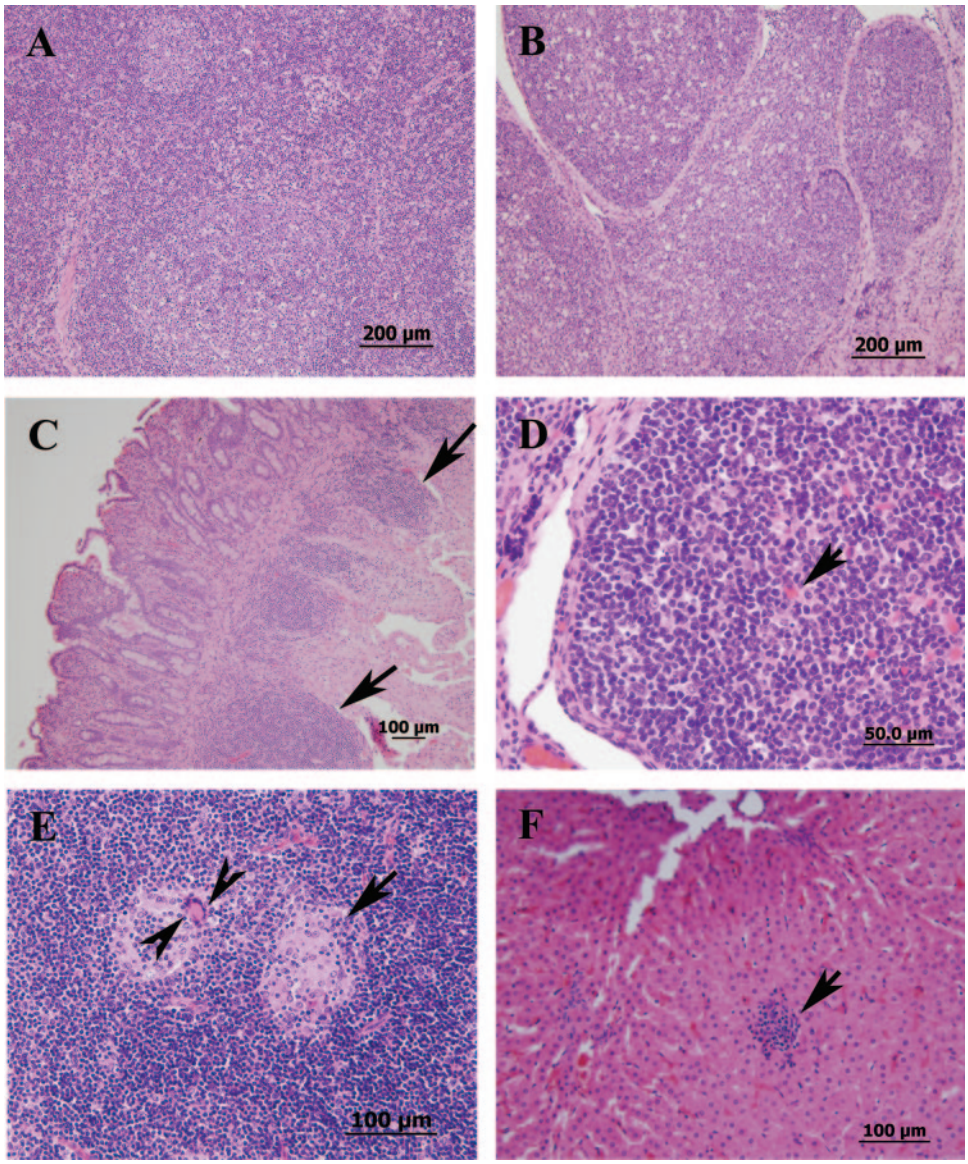

FIG. 3. Histopathology of calf tissues at different times following infection with *M. avium* subsp. *paratuberculosis* strain K-10. All sections were stained with hematoxylin and eosin. (A and B) Sections of a normal lymph node (A) and Peyer's patches of the ileum (B) from a control calf sacrificed 60 days after infection. (C) Small intestine with enlarged lamina propria (arrows) at 8 months postinfection. (D) Ileal Peyer's patches with large follicles and Mott cells (arrows) at 9 months postinfection. (E) Mesenteric lymph node with necrotic centers (arrow), scattered macrophages, and giant cells (arrowheads) at 9 months postinfection. (F) Liver with macrophage aggregate (arrow) at 9 months postinfection.

nize these organs to maintain the infection (Fig. 2). A close examination of the bacterial colonization pattern during the first 2 months of infection indicated that *M. avium* subsp. *paratuberculosis* colonized the intestine and the lymph nodes similarly. However, at later times, higher levels of *M. avium* subsp. *paratuberculosis* were found in the mesenteric lymph nodes, suggesting that colonization of this organ was preferred, especially as the infection progressed beyond 3 months. On the other hand, when we cultured fecal samples following the early stage of infection (first 4 days postinfection), we did not detect *M. avium* subsp. *paratuberculosis* bacilli even in samples collected 9 months postinfection, despite the considerable levels of *M. avium* subsp. *paratuberculosis* detected in the ileum.

Histopathology of infected animals. In addition to tissue colonization, we examined histological changes during persistent infection in *M. avium* subsp. *paratuberculosis*-infected calves. Analysis of tissues collected up to 3 months postinfection did not reveal any discernible lesions in *M. avium* subsp. *paratuberculosis*-infected animals compared to the PBS-inoculated control calf (Fig. 3A and B). In contrast, samples collected 6 months postinfection contained moderate numbers of lymphocytes, low numbers of plasma cells, abundant globular leukocytes, and scattered eosinophils and neutrophils in the lamina propria of the ileum. At 8 months postinfection, examination of small intestine sections revealed infiltrates containing moderate to marked numbers of eosinophils, lower

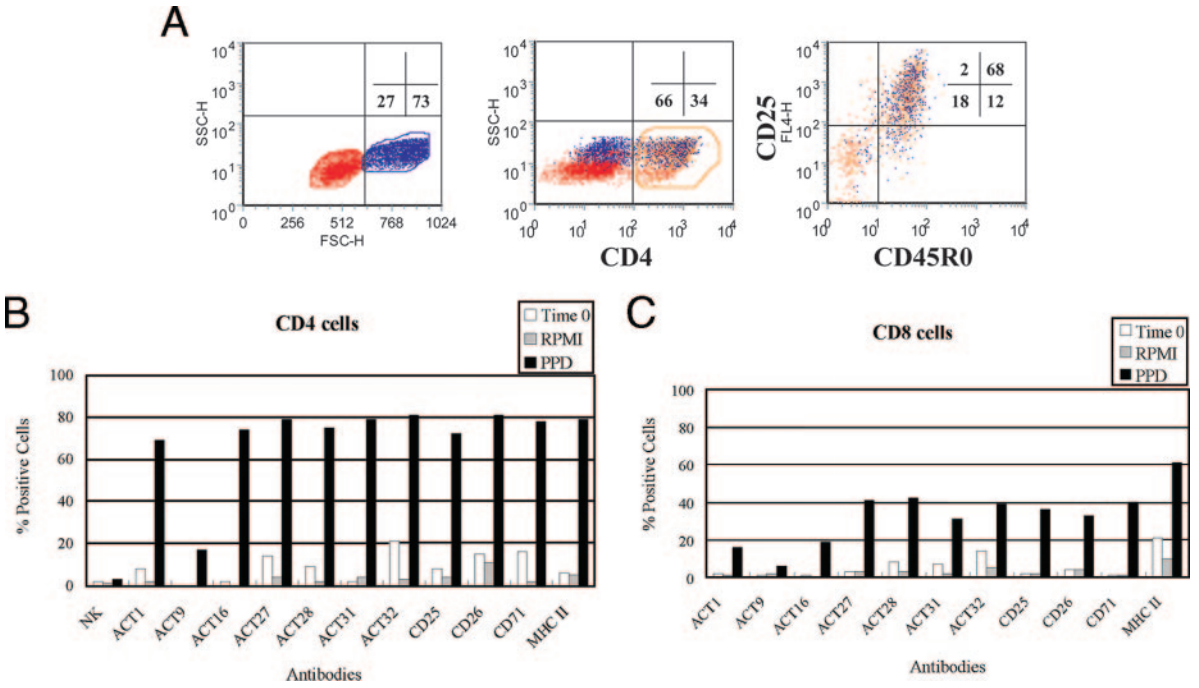

FIG. 4. Induction of cell-mediated immunity in calves after intestinal challenge with *M. avium* subsp. *paratuberculosis*. (A) Two-parameter dot plot profiles of PBMC stained with three MAbs specific for CD4, CD45R0 (memory T-cell marker), and CD25. Electronic gates were placed on small nonproliferating lymphocytes (left panel, side light scatter [SSC] versus forward light scatter [FSC], lower left quadrant) and large proliferating cells (right lower quadrant) to determine the relative proportions of small and large lymphocytes in the cell preparation. An additional electronic gate was placed on CD4 T cells (middle panel, circled area in lower right quadrant) to isolate all CD4 T cells for analysis and show the relative proportion of CD4 T cells present in the cell preparation. All three gates were used to analyze the expression of CD25 on CD4 naïve and memory T cells (right panel). This gating strategy was used to analyze expression of all the activation molecules on CD4 and CD8 memory T cells. (B) Summary of fluorescence-activated cell sorting analysis of CD4 memory T cells expressing MHC class II and activation molecules at time zero and 6 days after stimulation in RPMI medium alone or with PPD of *M. avium* subsp. *paratuberculosis*. The histogram shows the relative proportions of CD4 memory T cells expressing different activation molecules after 6 days of culture. (C) Summary of fluorescence-activated cell sorting analysis of CD8 memory T cells expressing different MHC class II and activation molecules.

numbers of globular leukocytes, lymphocytes, and plasma cells, and scattered mast cells throughout the lamina propria, with occasional involvement of the submucosa (Fig. 3C). Also, mild to moderate lymphoid hyperplasia was observed with the presence of hemosiderin-laden macrophages. All of the cells described above could be part of the host responses to early stages of infection with *M. avium* subsp. *paratuberculosis*. However, at 9 months postinfection, the ileal Peyer's patches were large and prominent (a characteristic of *M. avium* subsp. *paratuberculosis* infection) with large follicles with many lymphocytes that were prominent germinal centers, and many of the centers contained Mott cells (globulin-stuffed cells) (Fig. 3D). In some mesenteric lymph nodes, necrotic or apoptotic lymphocytic centers were found in addition to aggregates of macrophages with giant cell formation (Fig. 3E). Also, several nodular lymphoid aggregates occasionally admixed with macrophages were observed in liver sections (Fig. 3F), suggesting that there was a low level of mycobacterial colonization not detected by culturing. Nonetheless, no discernible acid-fast bacilli were present in the sections examined.

Cellular and humoral responses to early infection with *M. avium* subsp. *paratuberculosis*. To monitor the host responses following the interaction of *M. avium* subsp. *paratuberculosis* with ileal tissues, we used a panel of immunological assays designed to measure humoral and cellular responses. Whole blood samples were collected periodically from infected and control animals and used for ELISA and flow cytometric analyses. All samples of sera collected up to 9 months postinfection from infected animals were negative as determined by ELISA. Additionally, PPD skin tests performed 3 to 4 months following infection were negative for all animals, indicating that no cell-mediated immunity was detectable when the skin test was used. Also, a flow cytometric analysis performed with samples collected 1 to 2 h following inoculation did not reveal any difference between infected and control animals (data not shown). However, a flow cytometric analysis performed 8 and 9 months postinfection clearly indicated that infected animals developed an immune response to *M. avium* subsp. *paratuberculosis* antigens, unlike the control calf.

Flow cytometric analyses performed 8 and 9 months postinfection revealed that there was marked proliferation of CD4 T cells following stimulation with mycobacterial PPD (Fig. 4A). The responding cells exhibited increased expression of CD25, CD26, CD71, major histocompatibility complex (MHC) class II, and seven additional activation molecules whose specificity is not known yet (Fig. 4B). Although CD8 T cells were also activated, they comprised only a small portion of the proliferating cells. Not all of the activation molecules were upregulated on CD8 memory T cells (Fig. 4C). The γδ T cells accounted for ~40% of the cells in unstimulated and PPD-

stimulated cultures. These cells were present mainly in the small lymphocyte gate, indicating that they were not proliferating. However, they exhibited low-level expression of CD25. NK cells comprised ~11% of stimulated and unstimulated cultures. They were also present in the small lymphocyte gate, indicating that they were not activated. Cells from the control calf did not proliferate when they were cultured with PPD. Unfortunately, blood samples were not processed for flow cytometric analysis at earlier times (e.g., 3 to 4 months postinfection) to identify the earliest time that a proliferative response could be detected in comparison to the traditional skin test.

Localized responses to *M. avium* subsp. *paratuberculosis* infection. Because infected animals remained in the subclinical phase of JD (infected with no signs of the disease), we decided to examine the host microenvironment where *M. avium* subsp. *paratuberculosis* resides during this phase. To analyze the host responses to the presence of *M. avium* subsp. *paratuberculosis*, we used quantitative RT-PCR to obtain profiles of the expression of key cytokines (interleukin-4 [IL-4], gamma interferon [IFN-γ], tumor necrosis factor alpha [TNF-α], and IL-12) that are known to control the progression of JD in the ileum and lymph nodes (34). Generally, the cytokine levels were higher in the mesenteric lymph nodes (Fig. 5A) than in the intestine (Fig. 5B), probably because of the immune cell-rich environment in the lymph nodes. However, the cytokines expressed had different profiles depending on the type of tissue examined and the time of sampling following infection. In the lymph nodes, the levels of the transcripts of both IFN-γ and TNF-α increased substantially over time, while the levels of the transcripts of IL-4 decreased continuously at the same times (Fig. 5A). Moreover, the IL-12 levels were high at all times examined and were even higher at 9 months postinfection. In contrast, the levels of IL-4 and IL-12 were low in all intestinal samples, especially at 9 months postinfection (Fig. 5B). Only the level of IFN-γ was relatively high at 6 and 8 months postinfection, while the level of TNF-α was unchanged at all times examined. Generally, the cytokines associated with TH1 cell responses (IL-12, IFN-γ, and TNF-α) were all induced compared to the cytokine associated with TH2 cell responses (IL-4) (3), especially at 9 months postinfection. Interestingly, the levels of colonization of *M. avium* subsp. *paratuberculosis* in lymph nodes were unchanged despite the high levels of cytokines compared to the decreasing levels of *M. avium* subsp. *paratuberculosis* in the ileum (Fig. 5).

Invasiveness of *M. avium* subsp. *paratuberculosis* strains with different genetic backgrounds. Culturing of *M. avium* subsp. *paratuberculosis* from different tissues following the first few hours of deposition in the intestine indicated that there was rapid translocation of the *M. avium* subsp. *paratuberculosis* bacilli to the mesenteric lymph nodes (Fig. 1A). Recently, we identified several attenuated mutants of *M. avium* subsp. *paratuberculosis* using a high-throughput transposon mutagenesis protocol (30). One of these mutants did not colonize mouse tissue efficiently and had an insertion in the *gcpE* gene (13). The *gcpE* gene is a member of a 6.3-kb operon (Fig. 6A) and encodes a protein involved in biosynthesis of isoprenoid, an important target for drug development (17). We investigated the translocation of the *gcpE* mutant using the calf model which we developed in order to examine a possible mechanism

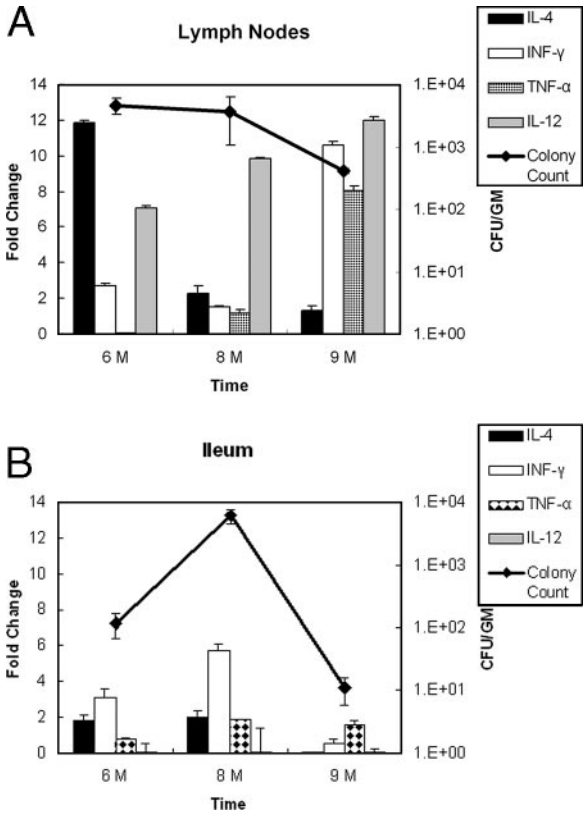

FIG. 5. Cytokine gene expression in calf tissues at different times following infection with *M. avium* subsp. *paratuberculosis*. Quantitative RT-PCR was used to examine the transcription of bovine cytokines (IL-4, IFN-γ, TNF-α, and IL-12). The fold changes in transcriptional levels in infected animals were estimated by comparison with the control calf tissue at 6, 8, and 9 months postinfection. Colony counts for the same tissues were also determined (*y* axis on the right). (A) Transcriptional profile of cytokines in mesenteric lymph nodes. (B) Transcriptional profile of cytokines in intestinal tissues.

of attenuation of this mutant. In this experiment, we estimated the colonization by the isogenic mutant (Δ*gcpE*) and compared this colonization to that of its parent strain, *M. avium* subsp. *paratuberculosis* wild-type strain ATCC 19698, using a competitive infection protocol (26). As expected, mesenteric lymph nodes collected 1 h postinoculation contained the wild-type strain (as determined by growth on Middlebrook 7H10 medium) but not the Δ*gcpE* strain (no growth on Middlebrook 7H10 medium supplemented with kanamycin), indicating that the Δ*gcpE* mutant was not able to translocate to the mesenteric lymph nodes. However, both the wild-type strain of *M. avium* subsp. *paratuberculosis* and the Δ*gcpE* mutant were detected in the liver and spleen samples, but the levels of the attenuated Δ*gcpE* mutant were much lower (Fig. 6B). The identities of the colonies retrieved were verified using a colony PCR protocol designed to examine the presence of the kanamycin marker gene in colonies retrieved from animal tissues (data not shown). Overall, the competitive index calculated for the mutant strain indicated that in all of the tissues examined the invasiveness of the mutant was significantly less than the invasiveness of the wild-type strain.

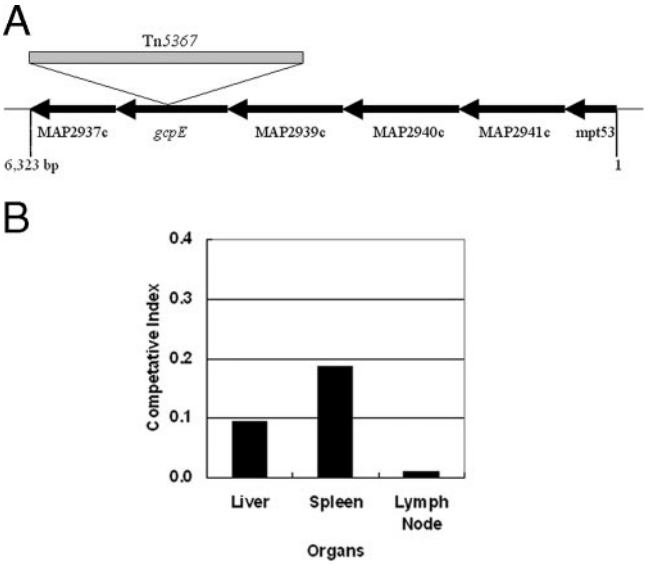

FIG. 6. (A) Diagram of the *gcpE* operon in *M. avium* subsp. *paratuberculosis*. The position of a Tn*5367* insertion present in the Δ*gcpE* mutant, as characterized in a previous study (30), is indicated. (B) Assessment of virulence of the Δ*gcpE* mutant using the intestinal calf model of paratuberculosis. The competitive index for the Δ*gcpE* mutant was calculated based on the levels of tissue colonization by the mutant strain and a virulent strain, *M. avium* subsp. *paratuberculosis* wild-type strain ATCC 19698.

DISCUSSION

Several bovine models for JD have been developed (18, 34, 35, 43) to study different aspects of infection with *M. avium* subsp. *paratuberculosis* and to analyze the host response to infection. In this study, we targeted the very early stages of infection, especially the subclinical stage of JD. Although in this study we examined cows for 9 months following infection, this period is considered an incubation phase for the chronic infection that usually manifests itself with chronic diarrhea and a decrease in the milk yield any time during the productive life span of dairy cows (5 to 10 years) (20). Specifically, we analyzed the first few hours and days following direct inoculation of a high dose of *M. avium* subsp. *paratuberculosis* into the ileum of susceptible calves. In this study, it was necessary to use surgical inoculation of animals in order to examine the very early stages of intestinal colonization and invasion; this route is unlike other routes of infection, such as oral and tonsillar deposition, in which the exact time of intestine-pathogen interaction cannot be determined. To our surprise, within 1 h of inoculation, the mycobacterial bacilli were able to traverse the intestinal barrier and reach the mesenteric lymph nodes, in contrast to the results of a previous study in which the organism took 5 to 20 h to traverse the intestinal barrier (22). Additionally, direct inoculation of *M. avium* subsp. *paratuberculosis* established persistent infections in both the ileum and the mesenteric lymph nodes, while *M. avium* subsp. *paratuberculosis* was not detected in the rest of the tissues (except in the jejunum of one calf), indicating the localized nature of infection, a fact that was confirmed by other workers (35). Previously, when the calf ileal loop model was used, both living and dead bacilli resided in macrophages lining the intestinal mucosa (22), and we have speculated that *M. avium* subsp. *paratuberculosis* uses intestinal macrophages to travel to the mesenteric lymph nodes. Tissue colonization data indicated that this transfer process is very rapid (within 1 h of inoculation) and very efficient (similar amounts of the inoculum were found in the lymph nodes and the ileum) and can be strain dependent. Previous models of JD (9, 15) suggested that ileal tissue plays an important role as a reservoir of infection. The mycobacterial colonization levels obtained here indicate that the mesenteric lymph nodes have an equal (if not greater) role in sustaining the persistent infection. Despite the fact that statistically significant differences in colonization were observed among some of the samples examined, we were not able to confirm that the bacteria localized to either the lymph nodes or intestine because of the low numbers of tissue samples analyzed. Nonetheless, more histological lesions associated with JD were observed in lymph nodes than in the ileum and other organs of infected calves. In naturally infected bulls, 75% of the mesenteric lymph nodes were positive for *M. avium* subsp. *paratuberculosis*, compared to only 25% of the intestinal tissues (1).

An unexpected outcome of the surgical model employed was the lack of fecal shedding following the first 3 days postinfection and up to the end of the experiment at 9 months postinfection despite the fact that both the BACTEC and MGIT culture systems were used. This lack of fecal shedding indicates that the animals did not enter the clinical phase of JD. Using the tonsillar deposition route of infection, intermittent fecal shedding was observed starting at 5 months postinfection (43), which is usually observed in naturally infected cows during clinical stages of JD. Unlike the direct deposition of *M. avium* subsp. *paratuberculosis*, it is possible that the tonsillar route of infection establishes a high level of intestinal colonization that leads to fecal shedding. In the tonsillar model of infection, the levels of intestinal colonization were not known so this possibility was not examined. Nonetheless, it is possible that infected animals could begin to shed *M. avium* subsp. *paratuberculosis* in their feces if samples are examined more than 9 months following direct deposition of *M. avium* subsp. *paratuberculosis* in the intestine.

During this experiment, profiles of both cellular and humoral responses were obtained to determine the host environment where *M. avium* subsp. *paratuberculosis* resides during the subclinical phase of JD. Using a commercial ELISA kit, no humoral responses were detected during the 9 months examined. However, utilizing a lipoarabinomannan-based ELISA, antibodies were detected as early as 4.4 months postinfection (43). This disparity could have been due to the lower sensitivity of the ELISA used in our study. Additionally, it is possible that the tonsillar route of infection used in the previous study (43) is actually more efficient in eliciting humoral immunity than our surgical deposition protocol. Usually, humoral responses can be detected in naturally infected cows when the clinical signs of the disease are evident (32). The cytokine profiles of the intestinal tissue and mesenteric lymph nodes revealed that there was predominant activation of cytokines characteristic of TH1-associated cellular responses and not TH2-associated humoral responses. This profile was consistent with the cytokine profiles associated with *M. avium* subsp. *paratuberculosis* in naturally infected cattle examined by other workers (10, 31), as

well as with the cytokine profiles associated with inflammatory bowl disease in humans (3). In contrast to the humoral responses, cellular immune responses to *M. avium* subsp. *paratuberculosis* were demonstrated by flow cytometric analysis and RT-PCR but not by the traditional skin test. It is noteworthy that the skin test was performed almost 4 to 5 months before the blood used for the flow cytometric analysis was collected. Additionally, both RT-PCR and flow cytometry analyses are more sensitive than skin tests for detection of cellular responses. As noted previously (13), there was a vigorous CD4 T-cell proliferative response to mycobacterial PPD in surgically infected animals. This response was characterized by upregulation of expression of MHC class II and $CD25^+$ $CD4^+$, consistent with the expression profile obtained previously for cattle in the subclinical phase of JD (44). Overall, expression of the activation molecules was variable in both CD4 and CD8 cell populations. Although γδ T cells exhibited low-level expression of CD25, based on cell size, they did not appear to be stimulated by PPD. Similarly, NK cells were present but were not activated. Both observations related to γδ T cells and NK cells could change as animals progress and develop clinical signs of JD. Generally, the presence of cellular immunity during the early phase of infection indicates that the animal is in the subclinical phase of JD and that cell-mediated immunity is important to the course of *M. avium* subsp. *paratuberculosis* infection (18, 44).

Finally, we took advantage of the mycobacterial translocation phenotype to develop a rapid assay for examining the virulence of *M. avium* subsp. *paratuberculosis* isolates with different genetic backgrounds. Using the invasion assay developed in this study, a mutant defective in expression of the *gcpE* gene was not able to traverse the intestinal barrier to the mesenteric lymph nodes, suggesting that the *gcpE*-encoded protein may have a role in mycobacterial survival and virulence. Using an antibody-based strategy, it was suggested that the 35-kDa membrane protein antigen could play a role in invasion of the epithelial cells by bacilli (2). A similar strategy could be used to further dissect the mechanism of *M. avium* subsp. *paratuberculosis* invasion with the assistance of the GcpE protein. Recently, several mycobacterial genes (e.g., *gcpE*, *fabG2_2*, *impA*, *papA2*, *pstA*, and *umaA1*) were implicated in facilitation of intestinal tissue colonization in a murine model of paratuberculosis (30). The intestinal invasion assay which we developed could play a key role in analyzing the contributions of such genes to different aspects of JD pathogenesis, such as invasion, colonization, and even persistence. In summary, despite the unusual route of inoculation, the surgical deposition of *M. avium* subsp. *paratuberculosis* in the calf ileum resulted in a good model that mimics several aspects of natural infection, such as the pattern of tissue colonization, persistence, and synchronized development of immune responses. This model was used to answer key questions related to mycobacterial virulence and pathogenesis, especially during very early stages of subclinical JD. The information obtained should improve our understanding of the nature of the host-pathogen interaction in mycobacterial infections.

ACKNOWLEDGMENTS

We acknowledge Gary Splitter and Bassam Abomoleak for reading the manuscript.

Research in the laboratory of A.M.T. was supported by the Animal Formula Fund (grant WIS04794) and the National Research Initiative of the USDA Cooperative State Research, Education and Extension Service (grant WIS04823 and Johne's Disease Integrated Program grant 2004-35605-14243), as well as by the TIF program of WARF.

REFERENCES

1. **Ayele, W. Y., M. Bartos, P. Svastova, and I. Pavlik.** 2004. Distribution of Mycobacterium avium subsp paratuberculosis in organs of naturally infected bull-calves and breeding bulls. Vet. Microbiol. **103:**209–217.
2. **Bannantine, J. P., J. F. J. Huntley, E. Miltner, J. R. Stabel, and L. E. Bermudez.** 2003. The *Mycobacterium avium* subsp. *paratuberculosis* 35 kDa protein plays a role in invasin of bovine epithelial cells. Microbiology **149:** 2061–2069.
3. **Bouma, G., and W. Strober.** 2003. The immunological and genetic basis of inflammatory bowel disease. Nat. Rev. Immunol. **3:**521–533.
4. **Cetinkaya, B., K. Egan, D. A. Harbour, and K. L. Morgan.** 1996. An abattoir-based study of the prevalence of subclinical Johne's disease in adult cattle in south west England. Epidemiol. Infect. **116:**373–379.
5. **Collins, M. T.** 1996. Diagnosis of paratuberculosis. Vet. Clin. N. Am. Food Anim. Pract. **12:**357–371.
6. **Collins, M. T., D. C. Sockett, W. J. Goodger, T. A. Conrad, C. B. Thomas, and D. J. Carr.** 1994. Herd prevalence and geographic distribution of, and risk factors for, bovine paratuberculosis in Wisconsin. J. Am. Vet. Med. Assoc. **204:**636–641.
7. **Committee on Diagnosis and Control of Johne's Disease, National Research Council.** 2003. Diagnosis and control of Johne's disease. National Academies Press, Washington, DC.
8. **Corn, J. L., E. J. B. Manning, S. Sreevatsan, and J. R. Fischer.** 2005. Isolation of *Mycobacterium avium* subsp. *paratuberculosis* from free-ranging birds and mammals on livestock premises. App. Environ. Microbiol. **71:** 6963–6967.
9. **Coussens, P. M.** 2004. Model for immune responses to *Mycobacterium avium* subsp. *paratuberculosis* in cattle. Infect. Immun. **72:**3089–3096.
10. **Coussens, P. M., N. Verman, M. A. Coussens, M. D. Elftman, and A. M. McNulty.** 2004. Cytokine gene expression in peripheral blood mononuclear cells and tissues of cattle infected with *Mycobacterium avium* subsp. *paratuberculosis*: evidence for an inherent proinflammatory gene expression pattern. Infect. Immun. **72:**1409–1422.
11. **Ellingson, J. L., C. A. Bolin, and J. R. Stabel.** 1998. Identification of a gene unique to *Mycobacterium avium* subspecies *paratuberculosis* and application to diagnosis of paratuberculosis. Mol. Cell. Probes **12:**133–142.
12. **Hamilton, H. L., A. J. Cooley, J. L. Adams, and C. J. Czuprynski.** 1991. Mycobacterium paratuberculosis monoassociated nude mice as a paratuberculosis model. Vet. Pathol. **28:**146–155.
13. **Hecht, S., W. Eisenreich, P. Adam, S. Amslinger, K. Kis, A. Bacher, D. Arigoni, and F. Rohdich.** 2001. Studies on the nonmevalonate pathway to terpenes: the role of the GcpE (IspG) protein. Proc. Natl. Acad. Sci. USA **98:**14837–14842.
14. **Hill, B. B., M. West, and K. V. Brock.** 2003. An estimated prevalence of Johne's disease in a subpopulation of Alabama beef cattle. J. Vet. Diagn. Investig. **15:**21–25.
15. **Hines, M. E., J. M. Kreeger, and A. J. Herron.** 1995. Mycobacterial infections of animals: pathology and pathogenesis. Lab. Anim. Sci. **45:**334–351.
16. **Kalis, C. H., J. W. Hesselink, H. W. Barkema, and M. T. Collins.** 2001. Use of long-term vaccination with a killed vaccine to prevent fecal shedding of *Mycobacterium avium* subsp. *paratuberculosis* in dairy herds. Am. J. Vet. Res. **62:**270–274.
17. **Kemp, L. E., C. S. Bond, and W. N. Hunter.** 2002. Structure of 2C-methyl-D-erythritol 2,4-cyclodiphosphate synthase: an essential enzyme for isoprenoid biosynthesis and target for antimicrobial drug development. Proc. Natl. Acad. Sci. USA **99:**6591–6596.
18. **Koo, H. C., Y. H. Park, M. J. Hamilton, G. M. Barrington, C. J. Davies, J. B. Kim, J. L. Dahl, W. R. Waters, and W. C. Davis.** 2004. Analysis of the immune response to *Mycobacterium avium* subsp. *paratuberculosis* in experimentally infected calves. Infect. Immun. **72:**6870–6883.
19. **Linnabary, R. D., G. L. Meerdink, M. T. Collins, J. R. Stabel, R. W. Sweeney, M. K. Washington, and S. J. Wells.** 2001. Johne's disease in cattle. Counc. Agric. Sci. Technol. **17:**1–10.
20. **Manning, E. J. B., and M. T. Collins.** 2001. Mycobacterium avium subsp. paratuberculosis: pathogen, pathogenesis and diagnosis. Rev. Sci. Tech. **20:** 133–150.
21. **Manning, E. J. B., H. Steinberg, V. Krebs, and M. T. Collins.** 2003. Diagnostic testing patterns of natural Mycobacterium paratuberculosis infection in pygmy goats. Can. J. Vet. Res. **67:**213–218.
22. **Momotani, E., D. L. Whipple, A. B. Thiermann, and N. F. Cheville.** 1988. Role of M cells and macrophages in the entrance of *Mycobacterium paratuberculosis* into domes of ileal peyer's patches in calves. Vet. Pathol. **25:**131–137.
23. **Munjal, S. K., B. N. Tripathi, and O. P. Paliwal.** 2005. Progressive immunopathological changes during early stages of experimental infection of goats

with *Mycobacterium avium* subspecies *paratuberculosis*. Vet. Pathol. **42:**427–436.
24. **Muskens, J., F. van Zijderveld, A. Eger, and D. Bakker.** 2002. Evaluation of the long-term immune response in cattle after vaccination against paratuberculosis in two Dutch dairy herds. Vet. Microbiol. **86:**269–278.
25. **Mutwiri, G. K., U. Kosecka, M. Benjamin, S. Rosendal, M. Perdue, and D. G. Butler.** 2001. *Mycobacterium avium* subspecies *paratuberculosis* triggers intestinal pathophysiologic changes in beige/scid mice. Comp. Med. **51:**538–544.
26. **Ruley, K. M., J. H. Ansede, C. L. Pritchett, A. M. Talaat, R. Reimschuessel, and M. Trucksis.** 2004. Identification of Mycobacterium marinum virulence genes using signature-tagged mutagenesis and the goldfish model of mycobacterial pathogenesis. FEMS Microbiol. Lett. **232:**75–81.
27. **Sangari, F. J., J. Goodman, M. Petrofsky, P. Kolonoski, and L. E. Bermudez.** 2001. *Mycobacterium avium* invades the intestinal mucosa primarily by interacting with enterocytes. Infect. Immun. **69:**1515–1520.
28. **Schmittgen, T. D., and B. A. Zakrajsek.** 2000. Effect of experimental treatment on housekeeping gene expression: validation by real-time, quantitative RT-PCR. J. Biochem. Biophys. Methods **46:**69–81.
29. **Schmittgen, T. D., B. A. Zakrajsek, A. G. Mills, V. Gorn, M. J. Singer, and M. W. Reed.** 2000. Quantitative reverse transcription-polymerase chain reaction to study mRNA decay: comparison of endpoint and real-time methods. Anal. Biochem. **285:**194–204.
30. **Shin, S. J., C.-W. Wu, H. Steinberg, and A. M. Talaat.** 2006. Identification of novel virulence determinants in *Mycobacterium paratuberculosis* by screening a library of insertional mutants. Infect. Immun. **74:**3825–3833.
31. **Stabel, J. R.** 2000. Cytokine secretion by peripheral blood mononuclear cells from cows infected with *Mycobacterium paratuberculosis*. Am. J. Vet. Res. **61:**754–760.
32. **Stabel, J. R., S. J. Welis, and B. A. Wagner.** 2002. Relationships between fecal culture, ELISA, and bulk tank milk test results for Johne's disease in US dairy herds. J. Dairy Sci. **85:**525–531.
33. **Storset, A. K., H. J. Hasvold, M. Valheim, H. Brun-Hansen, G. Berntsen, S. K. Whist, B. Djonne, C. M. Press, G. Holstad, and H. J. S. Larsen.** 2001. Subclinical paratuberculosis in goats following experimental infection. An immunological and microbiological study. Vet. Immunol. Immunopathol. **80:**271–287.
34. **Sweeney, R. W., D. E. Jones, P. Habecker, and P. Scott.** 1998. Interferon-gamma and interleukin 4 gene expression in cows infected with *Mycobacterium paratuberculosis*. Am. J. Vet. Res. **59:**842–847.
35. **Sweeney, R. W., J. Uzonna, R. H. Whitlock, P. L. Habecker, P. Chilton, and P. Scott.** 2006. Tissue predilection sites and effect of dose on *Mycobacterium avium* subsp. *paratuberculosis* organism recovery in a short-term bovine experimental oral infection model. Res. Vet. Sci. **80:**253–259.
36. **Talaat, A. M., S. T. Howard, I. W. Hale, R. Lyons, H. Garner, and S. A. Johnston.** 2002. Genomic DNA standards for gene expression profiling in *Mycobacterium tuberculosis*. Nucleic Acids Res. **30:**e104.
37. **Talaat, A. M., R. Reimschuessel, S. S. Wasserman, and M. Trucksis.** 1998. Goldfish, *Carassius auratus*, a novel animal model for the study of *Mycobacterium marinum* pathogenesis. Infect. Immun. **66:**2938–2942.
38. **Tanaka, S., M. Sato, T. Taniguchi, and Y. Yokomizo.** 1994. Histopathological and morphometrical comparison of granulomatous lesions in BALB/c and C3H/HeJ mice inoculated with *Mycobacterium paratuberculosis*. J. Comp. Pathol. **110:**381–388.
39. **Thornton, C. G., K. M. Maclellan, J. R. Stabel, C. Carothers, R. H. Whitlock, and S. Passen.** 2002. Application of the C_{18}-carboxypropylbetaine specimen processing method to recovery of *Mycobacterium avium* subsp. *paratuberculosis* from ruminant tissue specimens. J. Clin. Microbiol. **40:**1783–1790.
40. **Uzonna, J. E., P. Chilton, R. H. Whitlock, P. L. Habecker, P. Scott, and R. W. Sweeney.** 2003. Efficacy of commercial and field-strain *Mycobacterium paratuberculosis* vaccinations with recombinant IL-12 in a bovine experimental infection model. Vaccine **21:**3101–3109.
41. **Valentin-Weigand, P., and R. Goethe.** 1999. Pathogenesis of *Mycobacterium avium* subspecies *paratuberculosis* infections in ruminants: still more questions than answers. Microbes Infect. **1:**1121–1127.
42. **Valheim, M., A. K. Storset, M. Aleksandersen, H. Brun-Hansen, and C. M. Press.** 2002. Lesions in subclinical paratuberculosis of goats are associated with persistent gut-associated lymphoid tissue. J. Comp. Pathol. **127:**194–202.
43. **Waters, W. R., J. M. Miller, M. V. Palmer, J. R. Stabel, D. E. Jones, K. A. Koistinen, E. M. Steadham, M. J. Hamilton, W. C. Davis, and J. P. Bannantine.** 2003. Early induction of humoral and cellular immune responses during experimental *Mycobacterium avium* subsp. *paratuberculosis* infection of calves. Infect. Immun. **71:**5130–5138.
44. **Weiss, D. J., O. A. Evanson, and C. D. Souza.** 2006. Mucosal immune response in cattle with subclinical Johne's disease. Vet. Pathol. **43:**127–135.
45. **Whittington, R. J., and E. S. G. Sergeant.** 2001. Progress towards understanding the spread, detection and control of Mycobacterium avium subsp. paratuberculosis in animal populations. Aust. Vet. J. **79:**267–278.
46. **Wu, C.-W., J. Glasner, M. T. Collins, S. Naser, and A. M. Talaat.** 2006. Whole-genome plasticity among *Mycobacterium avium* subspecies: insights from comparative genomic hybridizations. J. Bacteriol. **188:**711–723.

Editor: V. J. DiRita